1P5-9

Effect of Transmission Patterns on 2C-3D Flow Vector Estimation with a 2D Matrix Array Transducer

Kei Mitsui[1‡], Kaya Takakusagi[1], Takuro Ishii[1,2], and Yoshifumi Saijo[1*] ([1]Grad. School of Biomed. Eng., Tohoku Univ.; [2]FRIS. Tohoku Univ.)

1. Introduction

Three-dimentional (3D) blood flow imaging using ultrasound enables quantitative evaluation of turbulant blood flow patterns such as that in the ascending aorta[1]. A solution to achieve such imaging is to use a multi-angle vector Doppler estimation[2,3] with a two dimentional (2D) matrix array transducer steering unfocused transmissions in both lateral and elevational directions. However, driving all the elements of this transducer simultaneously is too demanding for the data acquisition system. To overcome this problem, the transducer is connected to a 256-channels US scanner through a 4-to-1 multiplexer. In this case, the electric circuit pattern of the multiplexer limits the ultrasound transmission patterns. The multiplexer utilized in this study has a restriction that the 2D matrix array transducer can only steer the transmitted pulses along the lateral direction. In this study, we evaluated two possible transmission patterns under the restriction by comparing the performance of two-components-3D (2C-3D) flow estimations with the dual-angle vector Doppler estimation approach.

2. Methods

2.1 Experimental setup

We performed phantom experiments to evaluate the effect of the transmission patterns on 2C-3D flow vector estimation using a 2D matrix array transducer. As shown in **Fig. 1**, a 2D matrix array transducer (Vermon) consisted of 1024 (32 × 32) elements (fc: 3.47 MHz; element pitch: 0.3 mm) was utilized and connected to a programable ultrasound scanner (Vantage 256 system, Verasonics) through a 4-to-1 multiplexer (UTA 1024-MUX Adapter, Verasonics). The multiplexer had predefined sub-aperture groups, which were four 32×8 elements (Ap1~Ap4) divided along the elevational direction of the transducer. It enables the transducer to transmit with all elements simultaneously and receive with each of the four sub-apertures. Therefore, 3D data was obtained by transmitting and receiving four times in one transmission direction and accumulating the reconstructed data.

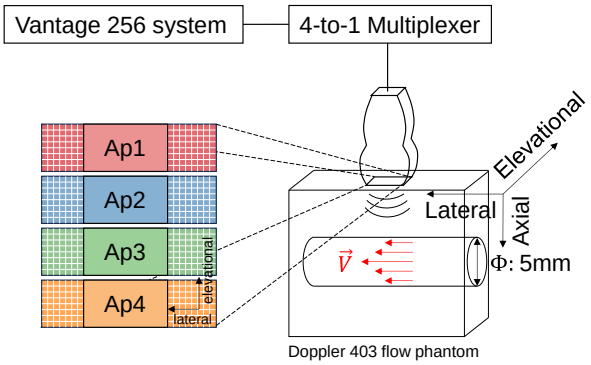

Fig. 1 Experimental setup and sub-apertures of the 2D matrix transducer.

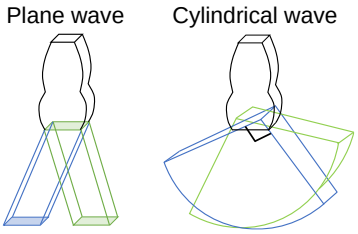

Fig. 2 Two transmission patterns used in this study (Left: Plane wave; Right: Cylindrical wave)

Fig. 2 shows two investigated transmission patterns, i.e., plane wave and cylindrical wave transmissions. Each transmission pattern was evaluated on 2C-3D flow vector estimation. For plane wave transmission, 15 transmissions were performed at steering angles of -7°~7° for B-mode imaging, followed by 32 alternating transmissions at steering angles of ±5° for dual-angle Doppler measurements. For cylindrical wave transmission, 15 transmissions were made at steering angles of -42°~42° for B-mode imaging, followed by 32 alternating transmissions at steering angles of ±30° for dual-angle Doppler measurements. The central angle of the cylindrical wave was set at 90°. Note that all the steering angles were in the lateral direction due to the restriction of the multiplexer. The transmission frequency for both transmissions was 3.47 MHz, and the pulse repetition frequency (PRF) was set at 9.6 kHz. However, since 8 transmissions were performed in 1 frame, the actual PRF was 1.2 kHz.

‡mitsui.kei.t3@dc.tohoku.ac.jp
*saijo@tohoku.ac.jp

2.2 2D flow vector estimation

1D flow velocities (v_1, v_2) for respective transmission steering angles were estimated from the acquired data using the singular value decomposition (SVD) clutter filtering and the autocorrelation methods. Then, 2D flow vector ($V_{lateral}, V_{axial}$) was obtained from the estimated 1D flow velocities (v_1, v_2) by the following equation[2]:

$$\frac{1}{2}\begin{bmatrix} sin\theta_1 + sin\varphi_1 & cos\theta_1 + cos\varphi_1 \\ sin\theta_2 + sin\varphi_2 & cos\theta_2 + cos\varphi_2 \end{bmatrix}\begin{bmatrix} V_{lateral} \\ V_{axial} \end{bmatrix} = \begin{bmatrix} v_1 \\ v_2 \end{bmatrix} \quad (1)$$

where (θ_1, θ_2) are the angles between the axial axis and the direction of the transmitted pulses in the 2 directions, and (φ_1, φ_2) are the angles between the axial axis and the direction of received signals for each transmission.

3. Results and discussion

The 2C-3D flow vectors were estimated using plane wave and cylindrical wave transmissions, respectively. In **Figure 3**, **(a-1) and (a-2),** and **(b-1) and (b-2)** show the 2C-3D flow vector images and $V_{lateral}$ in the short axis plane, respectively. For both transmission methods, flow vectors with high velocities at the center of the channel were estimated. The 10-frames mean and standard deviation (SD) of $V_{lateral}$ on the elevational diameter are displayed in **Fig. 3 (c-1) and (c-2)**. Root mean squared errors (RMSE) was 87.2 mm/s for plane wave transmission and 142.9 mm/s for cylindrical wave transmission. The temporal SD was 70.21 mm/s for plane wave transmission and 55.79 mm/s for cylindrical wave transmission. These results indicate that the dual-angle Doppler estimator allows 2C-3D flow vector estimation with both transmission patterns. In addition, plane wave transmission provides a velocity estimation closer to the theoretical value than cylindrical wave transmission. In the future study, we plan to identify the optimal transmission pattern.

4. Conclusion

In this paper, we achieved 2C-3D flow vector estimation using plane wave and cylindrical wave transmissions with a 2D matrix array transducer and a 4-to-1 multiplexer and evaluated the effect of transmission patterns on the vector estimation accuracy. The experiment indicated that plane wave transmission has a higher estimation accuracy than that of cylindrical wave transmission.

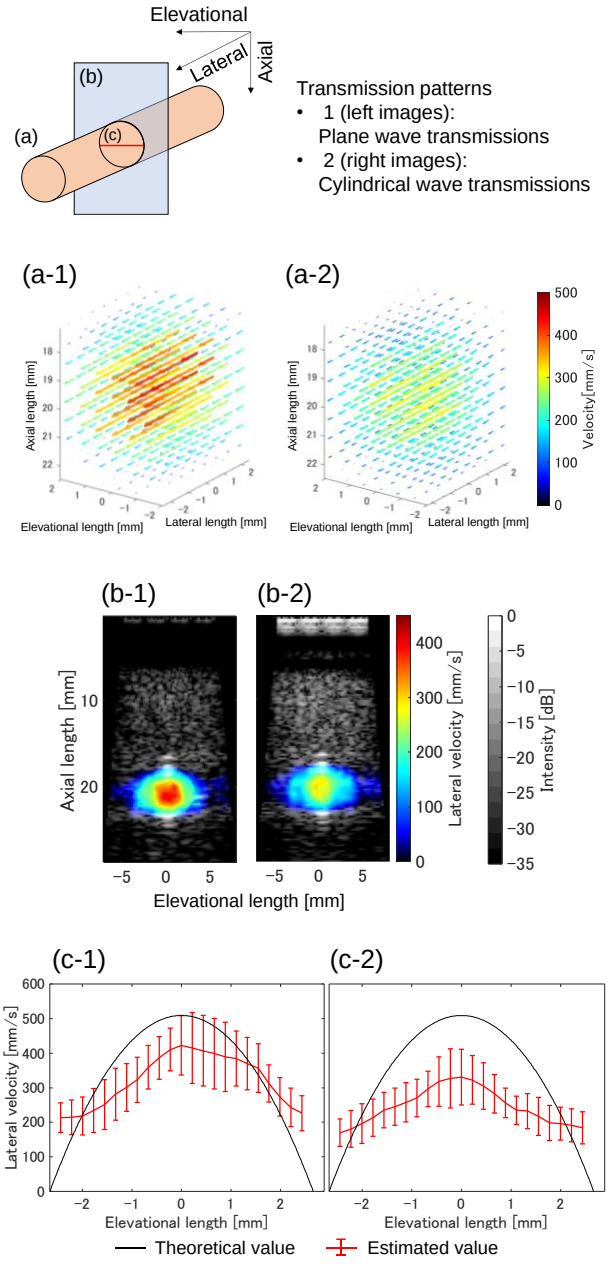

Fig. 3 Results of 2C-3D flow vector estimation using plane wave transmissions (left images) and cylindrical wave transmissions (right images).
(a) 2C-3D flow vector images
(b) Lateral flow velocity in the short axis plane
(c) Lateral flow velocity on the elevational diameter (Error bars: temporal standard deviation). Black lines show the theoretical profiles.

References

1) M. Correia, J. Provost, M. Tanter, and M. Pernot: Phys. Med. Biol. 61 (2016) L48–L61
2) B. Y. S. Yiu and A. C. H. Yu: IEEE Trans. Ultrason. Ferroelectr. Freq. Control 63 (2016) p.1733-1744.
3) M. Maeda et al.: Jpn. J. Appl. Phys. 57 (2018) 07LF02-1.